Vibrationally Excited OD Radicals from the Reaction of Oxygen Atoms with Chemisorbed Deuterium on Tungsten

H. K. Shin

Department of Chemistry,† University of Nevada, Reno, Nevada 89557

Received: October 1, 1997; In Final Form: December 30, 1997

The possibility of producing highly excited OD radicals in the reaction of gas-phase atomic oxygen with deuterium chemisorbed on a tungsten surface has been explored using classical trajectory procedures. The many-body nature of the gas−surface reaction is explicitly considered in constructing a potential energy surface. Nearly all reactive events occur in a direct collision on a subpicosecond scale. The vibrational population distribution of OD radicals is found to be inverted, with the highest population appearing at vibrational level 6. The Eley−Rideal mechanism can account for these results. The calculations are carried out at the gas and surface temperatures of 1000 and 300 K, respectively, where the probability of OD formation is 0.12.

I. Introduction

The system of hydrogen atoms chemisorbed on a tungsten surface is one of the most widely studied adatom moieties.[1−17] Since chemisorption energies for hydrogen atoms on a close-packed metal surface lie in the range 2−3 eV,[18,19] there can be a large amount of energy released in the reaction of an energy-rich gas-phase reactant with such an adatom−surface system. For reactants such as hydrogen and oxygen, the bond formed between the gas atom and the adatom is 4−5 eV, so the reaction exothermicity is about 2 eV, which is distributed in various modes of the product state. Therefore, a hydrogen-covered metal surface is an attractive reactive site for producing vibrationally excited products.[6,7,10,13,14,16] For the reaction involving deuterium, the vibrational excitation of OD can be high because of a lower frequency of the OD vibration compared with that of OH;[17] thus reaction of O and D on a metal surface promises to be an attractive way of generating excited radicals. When such excited species are used in subsequent steps, the desired reaction can proceed at an enhanced rate, in which case metal−surface catalytic activity may be interpreted in terms of not only the traditional concept of surface site specificity but also the participation of energy-rich intermediates.

The purpose of this paper is to study the possibility of generating vibrationally excited OD radicals in the reaction of gas-phase atomic oxygen with deuterium chemisorbed on a tungsten surface, O(g) + D(ad)/W → OD(g) + W. We solve the equations of motion obtained by uniting the gas-phase reaction dynamics approach and generalized Langevin theory[20−23] for the displacements and conjugated momenta of interacting atoms in the primary system. We include the gas−adatom interaction, gas−surface layer atom interactions, and vibrational motions of inner solid atoms in the formulation of a potential energy surface. The incident gas atom to adatom interaction is under the influence of forces exerted by all these surface-layer atoms and a chain of many inner atoms that connects the reaction zone to the heat bath. We consider the reaction to take place at the gas temperature of 1000 K and the surface temperature of 300 K.

† Theoretical Chemistry Group Contribution No. 1165.

II. Interaction Potentials and Numerical Procedures

The interaction model and numerical procedures have already been reported elsewhere.[17] We recapitulate the essential aspects here. The deuterium D is chemisorbed on the surface site W_0, which is surrounded by eight top layer (001) atoms (W_i, i = 1−8) and four body-centered atoms (W_j, j = 1−4) of four unit cells. Then, the center atom W_0 is the atom common to all four unit cells. These W_i atoms are at $\phi = {}^1/_4(i-1)\pi$ around the adatom−surface axis, and W_j atoms are at $\phi = {}^1/_4(2j-1)\pi$. In addition, the center atom W_0 interacts with the N-atom chain that links the reaction zone to the heat bath such that the chain provides a simple quasiphysical picture of energy flow between the reaction zone and the heat bath. The incident gas-phase oxygen atom approaches the surface with an angle θ to and an azimuthal angle ϕ around the D−W_0 axis, which is considered to be in the surface normal direction, at the impact parameter b. A total of six degrees of freedom is needed to describe the motions of O(X,Y,Z) and D(x,y,z) atoms on the surface, where $X = b\cos\phi$, $Y = b\sin\phi$, and Z determines the O-to-surface distance. For the adatom−surface bond vibrating in the direction of the surface normal, we take z as the D−W_0 bond distance (z_{DW_0}) and $x = y = 0$. The O-to-D distance is $z_{OD} = (Z - z_{DW_0})/\cos\theta$ and the O-to-W_i, O-to-W_j distances are dependent on Z, z_{DW_0}, θ, and ϕ. The coordinate of the center atom is denoted by ξ_0 and those of the N-chain atoms by ξ_1, ξ_2, ..., ξ_N. All these N-chain atoms and W_i, W_j surface atoms interact directly with the reaction zone, which consists of O, D, and W_0 atoms. In the model, all these atoms belong to the primary system. We then designate the remaining infinite number of solid atoms beyond the N-atom chain as secondary atoms, which influence the dynamics of the primary system through dissipative and stochastic forces. These two forces balance, according to the fluctuation−dissipation theorem, so that the proper temperature is maintained in the primary zone.[22] Thus, we reduce the original many-body problem to a manageable size consisting of three reaction-zone atoms, 12 surface atoms, and N chain atoms, where N is typically about 10.[24] Here, the Nth atom is subject to dissipative and stochastic forces.

To construct a rigorous form of the potential energy surface, we include OD, DW_0, nine OW_i (including $i = 0$), and four

S1089-5639(97)03190-3 CCC: $15.00
Published on Web 03/07/1998

OW_j atom−atom interaction terms in the London−Eyring−Polanyi−Sato formulation. An important modification to the standard LEPS procedure[3,4] is the introduction of the Coulomb Q_{OS} and exchange A_{OS} terms of many O-to-surface atom (OS) interactions defined as

$$Q_{OS} + A_{OS} = D_{OS}\left\{\sum_{i=0}^{8}[e^{(z_{ei}-z_i)/a_{OS}} - 2e^{(z_{ei}-z_i)/2a_{OS}}] + \sum_{j=1}^{4}[e^{(z_{ej}-z_j)/a_{OS}} - 2e^{(z_{ej}-z_j)/2a_{OS}}]\right\} \quad (1a)$$

$$Q_{OS} - A_{OS} = \frac{D_{OS}(1-\Delta_{OS})}{2(1+\Delta_{OS})}\left\{\sum_{i=0}^{8}[e^{(z_{ei}-z_i)/a_{OS}} + 2e^{(z_{ei}-z_i)/2a_{OS}}] + \sum_{j=1}^{4}[e^{(z_{ej}-z_j)/a_{OS}} + 2e^{(z_{ej}-z_j)/2a_{OS}}]\right\} \quad (1b)$$

Here the first sum in each equation contains the interaction between the gas atom and nine W_i atoms in the top layer, whereas the second sum is for that between O and four W_j atoms in the body-centered layer. For OD and DW_0 interactions, the corresponding terms are

$$Q_k + A_k = D_k[e^{(z_{e,k}-z_k)/a_k} - 2e^{(z_{e,k}-z_k)/2a_k}] \quad (2a)$$

$$Q_k - A_k = {}^1/_2 D_k[(1-\Delta_k)/(1+\Delta_k)][e^{(z_{e,k}-z_k)/a_k} + 2e^{(z_{e,k}-z_k)/2a_k}], \quad k = \text{OD, } DW_0 \quad (2b)$$

In the exponential parts of eq 1 and 2, the subscript "e" represents the equilibrium distance of the atom pair indicated. These distances and other pertinent potential parameters (D_k, a_k) are given in ref 17. The Sato parameters Δ's are adjusted until they minimize the barrier height and the attractive well in the product channel. The values are found to be $\Delta_{OD} = 0.49$, $\Delta_{DW_0} = 0.54$, and $\Delta_{OS} = 0.55$. We introduce the above energy terms in the LEPS expression

$$U = Q_{OD} + Q_{DW_0} + Q_{OS} - [A_{OH}{}^2 + A_{HW_0}{}^2 + A_{OS}{}^2 - A_{OD}A_{DW_0} - (A_{OD} + A_{DW_0})A_{OS}]^{1/2} \quad (3)$$

In the present system, the gas−surface vibration is directly coupled to the N-atom chain, a fictitious nearest-neighbor linear harmonic chain with the vibrational energy $V(\xi_n) = {}^1/_2 M_S \omega_{en} \xi_n{}^2$, where M_S is the mass of W and ω_{en} are the Einstein frequencies. Because of coupling, the sum of solid interaction potential energies includes cross terms such as ${}^1/_2 M_S \omega_{cn}{}^2 \xi_{n-1}\xi_n$, ${}^1/_2 M_S \omega_{c,n+1}{}^2 \xi_n \xi_{n+1}$, etc., where ω_{cn} are the coupling constants characterizing the chain. The values of ω_{en} and ω_{cn} are known.[24] Thus, with the LEPS function given above, we can express the overall interaction potential in the form

$$U(\{q\},\{z\},\{\xi\}) = U + \sum_n ({}^1/_2 M_S \omega_{en}{}^2 \xi_n{}^2 + {}^1/_2 M_S \omega_{cn}{}^2 \xi_{n-1}\xi_n + {}^1/_2 M_S \omega_{c,n+1}{}^2 \xi_n \xi_{n+1}) \quad (4)$$

where we use abbreviations $\{q\} = (Z, z_{DW_0}, \theta, \phi)$, $\{z\} = (z_i, z_j)$ for $j = 0, 1, ..., 8$, $j = 1, 2, 3, 4$, and $\{\xi\} = (\xi_0, \xi_1, \xi_2, ..., \xi_N)$.

We set up the equations of motion $m_i d^2q_i/dt^2 = -\partial U(\{q\}, \{z\},\{\xi\})/\partial q_i$ for $q_1 = Z$, $q_2 = z_{DW_0}$, $q_3 = \theta$, and $q_4 = \phi$, where m_i represents the corresponding reduced mass or moment of inertia. In integrating the equation $I d^2\theta(t)/dt^2 = -\partial U(\{q\},\{z\}, \{\xi\})/\partial\theta$ for the rotation of OD, it is important to recognize that OD forms after the turning point (t_{TP}) in a reactive event, where I is the moment of inertia of OD. Thus we begin the integration of the equation at this instance with $\theta(t_{TP})$, which is the solution of the angular velocity equation $d\theta(t)/dt = (2E/\mu)^{1/2} b/z_{OD}(t)^2$ at $t = t_{TP}$. Here E is the collision energy and μ is the reduced mass of the collision system. Since the O-to-D distance is strongly dependent on the interaction potential during the approach of the gas atom toward the adatom, we use the angular velocity equation rather than random sampling to determine θ-(t_{TP}). On the other hand, the initial azimuthal direction of the gas atom toward the surface needed in solving $I d^2\phi(t)/dt^2 = -\partial U(\{q\},\{z\},\{\xi\})/\partial\phi$ is taken to be $\phi = 2\pi l$, where l is a random number with a flat distribution in the closed interval (0,1). The initial conditions for Z and z_{DW_0} are shown elsewhere.[16] In addition to these equations, we introduce a set of equations describing the motions of all chain atoms ($n = 0-N$) according to the generalized Langevin formulation,[21,22]

$$M_S \ddot{\xi}_0(t) = -M_S \omega_{e0}{}^2 \xi_0(t) + M_S \omega_{cl}{}^2 \xi_1(t) - \partial U(\{q\},\{z\},\{\xi\})/\partial\xi_0 \quad (5a)$$

$$M_S \ddot{\xi}_n(t) = -M_S \omega_{en}{}^2 \xi_n(t) + M_S \omega_{cn}{}^2 \xi_{n-1}(t) + M_S \omega_{c,n+1}{}^2 \xi_{n+1}(t), \quad n = 1, 2, ..., N-1 \quad (5b)$$

$$M_S \ddot{\xi}_N(t) = -M_S \Omega_{c,N}{}^2 \xi_N(t) + M_S \omega_{c,N}{}^2 \xi_{N-1}(t) - M_S \beta_{N+1} \xi_N(t) + M_S f_{N+1}(t) \quad (5c)$$

where Ω_N is the adiabatic frequency. Therefore, at short times the nth oscillator responds like an isolated harmonic oscillator with frequency ω_{en}, whereas Ω_N determines the long-time response of the heat bath. The friction coefficient β_{N+1} governs the dissipation of energy to the heat bath. The term $M_S f_{N+1}(t)$ in eq 5c is governed by the fluctuation−dissipation theorem $\langle f_{N+1}(t)\, f_{N+1}(0)\rangle = (6kT_s/M_S)\beta_{N+1}\delta(t)$.[21,22] These friction and random forces are introduced in the last equation to represent the effects of the heat bath on the primary system. We solve the set of all these equations simultaneously for specified initial conditions[17] using the parameters ω_{en}, ω_{cn}, β_n, and Ω_N for solid vibrations shown in ref 16. The Debye temperature needed in solving eq 2 is known to be 400 K.[17] The collision energy distribution is assumed to be Maxwellian at a gas temperature of 1000 K. The surface temperature will be set at 300 K.

III. Results and Discussion

Gas atoms were initially located above the surface at $Z(t_0) =$ 15 Å. During the collision, the reaction-zone atoms form a weak O···D bond, while the D−W_0 bond weakens. Here, a dotted line is used between O···D to emphasize the nascent nature of the newly formed bond between O and D in the short-lived complex O···D−W_0. When the D−W_0 bond receives an energy exceeding its dissociation threshold D_{DW_0} from the O to D interaction and when D does not return to the surface after traveling into the gas phase at least 10 Å, we consider bond dissociation to have occurred. We will follow the rebounding O···D for a sufficiently long time to confirm that it has stabilized to the final product OD without trapping or redissociation.

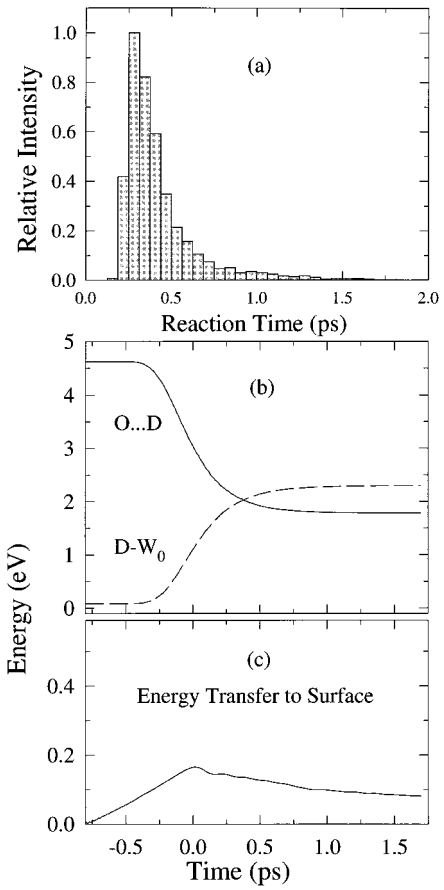

Figure 1. (a) Distribution of reaction times for the ensemble of single-impact collisions, (b) the ensemble-averaged C···D interaction and D−W_0 vibrational energies, and (c) the ensemble-averaged energy transfer to surface. In b, after reaction, the O···D curve remains at the OD vibrational energy, whereas the D−W_0 curve remains at the dissociation threshold, D_{DW_0}.

Throughout this work, we take the 10-atom chain, the length that we have established from a convergence test of energy transfer to the surface as a function of N. The probability of OD formation P_{OD}, defined as the ratio of the number of reactive trajectories to the total number of trajectories sampled (30 000), is 0.120 at $T_g = 1000$ K and $T_s = 300$ K. Some general features of the reaction under these thermal conditions are summarized in Figure 1. Figure 1a shows that nearly 95% of all reactive events occur at reaction times shorter than 1 ps in a single-impact collision. The reaction time measures the duration from the instant of impact to the time at which the D−W_0 bond has displaced 5 Å from its equilibrium bond distance in a reactive event. Such direct mode reactive events can be understood in terms of the Eley−Rideal (ER) mechanism, where incident gas atoms interact with adsorbed atoms and the gas reactant is not in equilibrium with the surface. The maximum intensity of the distribution of these short reaction times occurs near 0.3 ps. The exothermicity of O + D → OD is 4.45 eV,[25] which is the primary driver for D extraction from the surface. Then the depth of the well for OD is 4.45 + $^1/_2\hbar\omega_{OD}$ = 4.62 eV, where the OD fundamental is 2720 cm^{-1}.[25] The D−W_0 interaction energy is taken to be $D_{DW_0} = 2.30$ eV.[17] The ensemble average of all these subpicosecond events gives the value of 1.78 eV for the vibrational energy deposited in product radicals (see Figure 1b), indicating that most of the reaction energy is deposited in the product vibration. Figure 1b shows a rapid decrease of the ensemble-averaged O···D energy $\langle E_{v,OD}\rangle$ from D_{OD} to 1.78 eV as the time increases, whereas the D−W_0 vibrational energy $\langle E_{v,DW_0}\rangle$ rises from the initial value determined by the Boltzmann distribution at $T_s = 300$ K to the dissociation threshold D_{DW_0}. In Figure 1c, we show the time evolution of ensemble-averaged energy transfer to the surface, which indicates the N-atom chain gaining about 0.15 eV of the reaction energy and transferring it to the bulk phase. This dissipation process is very slow, continuing long after the reaction has completed. The result that the solid shares only a small fraction of the reaction exothermicity is a consequence of the large discrepancy between the masses of D and W. In fact, in O(g) + CO(ad)/Pt, where $m_{CO}/m_{Pt} = 0.144 \gg m_D/m_W = 0.011$, the amount of energy transfer is as large as 0.60 eV even at $T_g = 300$ K and $T_s = 0$ K.[24] We note that the Boltzmann sampling of D−W_0 vibrational energies at $T_s = 300$ K gives 99.8% of the total population in the $v_{DW_0} = 0$ state. Thus, in the Boltzmann sampling of 30 000 initial conditions at $T_s = 300$ K, essentially all D−W_0 vibrations are in the ground state with energy $E^0_{v,DW_0} = {}^1/_2\hbar\omega_{DW_0} = 0.080$ eV. In the following discussion of the calculated results obtained for the D−W_0 vibration at $T_s = 300$ K, we thus regard setting $v_{DW_0} = 0$ (i.e., $E^0_{v,DW_0} = 0.080$ eV) as equivalent to the Boltzmann sampling of the initial D−W_0 vibration.

Figure 2a shows the dependence of the OD vibrational energy $E_{v,OD}$ of all product radicals on the impact parameter for the initial D−W_0 vibrational energy fixed at $E_v{}^0{}_{,DW_0} = 0.080$ eV (i.e., at the $v_{DW_0} = 0$ state). A remarkable result seen in the figure is the complete absence of vibrationally low-lying radicals at the impact parameter below 1 Å. In $b \approx 0$ collisions, no OD with vibrational energy less than 2.2 eV is produced. From the eigenvalue expression $E_{vib}(v_{OD}) = hc\omega_e(v_{OD} + {}^1/_2) - hc\omega_e x_e(v_{OD} + {}^1/_2)^2$, with $\omega_e = 2720$ cm^{-1} and $\omega_e x_e = 44.05$ cm^{-1},[25] we find that the OD vibrational energy of 2.2 eV corresponds to level 7. As the impact parameter increases, the vibrational energy of OD decreases, but the excitation remains significant until b reaches 1.0 Å, where low-energy radicals suddenly appear. Including the latter range, there are three distinct ranges of b for OD formation. Also plotted in Figure 2a is the b-dependent probability of OD formation, $P_{OD}(b)$, which is highly structured, with the peaks corresponding to the three regions. This probability is defined as the ratio of the number of reactive trajectories to the number of trajectories sampled at a given b.

In $b \approx 0$ collisions, where the gas atom is incident more or less on top of the adatom atom, the product OD is in a highly excited state, but the extent of reaction is very small. The perturbation of the longitudinal vibration is efficient in such a collinear or near-collinear configuration (O···D−W_0), causing an efficient flow of energy from the O···D interaction to the D−W_0 vibration. However, when the gas atom rebounds from the adatom, it also efficiently takes back part of the energy from the D−W_0 vibration before the D−W_0 bond had a chance to dissociate. The amount of energy retaken by the rebounding atom is large enough to lower the energy of the D−W_0 bond below its dissociation threshold D_{DW_0}, thus preventing the bond dissociation. In a small fraction of these collisions occurring in a short reaction time, however, the energy-rich D−W_0 bond has a chance to dissociate before the energy flows back to the rebounding gas atom, in which case the reaction occurs and OD now recedes from the surface with a large amount of vibrational energy.

In the intermediate range $b = 0.4-0.8$ Å, where the extent of reaction is very large, vibrational excitation is still significant, especially at the lower end of the range (see Figure 2a). At the instant of a gas−surface impact in this range, where the gas-to-adatom direction is oriented by the angle $\theta = \tan^{-1}[b/(Z -$

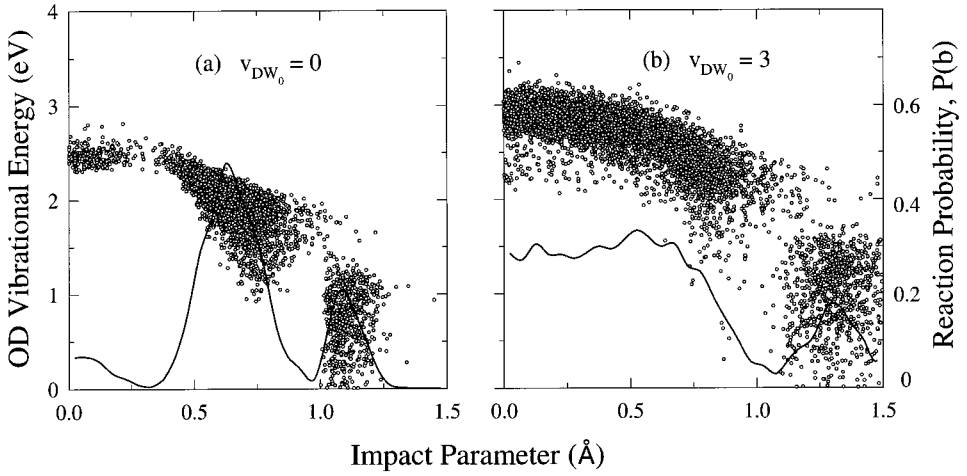

Figure 2. Dependence of the OD vibrational energy (open circles) on the impact parameter for the initial D−W_0 vibrational energy corresponding to (a) $v_{DW_0} = 0$ and (b) $v_{DW_0} = 3$. Also shown is the dependence of the reaction probability $P_{OD}(b)$ on the impact parameter (see the curve). The left-ordinate scale indicates the OD vibrational energy, and the right-ordinate scale is the reaction probability.

z_{DW_0})] from the D−W_0 axis, the O···D distance is somewhat shorter than the equilibrium bond distance of $z_{e,OD} = 0.97$ Å. Since z_{e,DW_0} is 1.67 Å, the equilibrium position of the adatom from the surface is about 2.6 Å, which is significantly shorter than $z_{e,HS} = 4.0$ Å. Therefore, the gas atom is likely to turn around from the surface at a distance significantly larger than 2.6 Å due to the repulsive potential wall created by many surface atoms. In such an oriented O-to-D interaction, energy flow to the D−W_0 vibration and then the return of energy back to the O···D interaction are less efficient than the collinear case. Consequently, a lesser amount of energy goes into the D−W_0 vibration, but the energy resides in the D−W_0 bond for a longer period, favoring its dissociation.

In the range $b = 1.0-1.2$ Å shown in Figure 2a, the O···D interaction is not very strong and only those gas atoms with a large translational energy can reach the impact region, where O···D is in a near-flat configuration on the surface. In these large-b collisions, the O···D direction is nearly perpendicular to the D−W_0 direction, but this configuration is not very efficient for vibrational energy transfer. Consequently, the extent of reaction is significantly lower than that in the intermediate-b range. In reactive events taking place at such a large b, a significant portion of the reaction energy now deposits in the OD rotation. As shown in Figure 2a, the reaction finally ceases for $b > 1.5$ Å, which is about halfway between the two surface sites (i.e., $\approx {}^1/_2 d_{WW}$). The nearest tungsten−tungsten distance d_{WW} is known to be 3.16 Å.[4]

If initially the D−W_0 bond had a larger amount of the vibrational energy, the reaction probability P_{OD} can be large even in $b \approx 0$ collisions because the D−W_0 bond now requires a smaller amount of energy from the incident atom for dissociation. Figure 2b for the initial D−W_0 vibrational excitation of 0.560 eV corresponding to the $v_{DW_0} = 3$ state clearly shows this result. The general features of this case are significantly different from those of the $v_{DW_0} = 0$ case shown in Figure 2a. Furthermore, the reaction probability P_{OD} is now 0.204, which is about 1.7 times the $v_{DW_0} = 0$ value. Thus, the influence of increasing the vibrational energy of the adatom−surface bond on the OD formation in the present exothermic reaction over an early barrier is significant. However, a more interesting result is that the extent of product vibrational excitation is now increased approximately by the amount of the vibrational energy initially present in the D−W_0 bond over the $v_{DW_0} = 0$ case. This result clearly indicates that the initial excitation of the D−W_0 vibration remains in the bond during energy transfer from O···D to D−W_0. Another interesting result is that the extent of reaction is large over the wide range $b = 0-0.8$ Å, where the b-dependent reaction probability is essentially constant. Beyond this b range, the b-dependent reaction probability varies similar to that of the $v_{DW_0} = 0$ case, although the high-b end is now pushed toward a large value of $b = 1.5$ Å. Some reactive events occur at an impact parameter larger than 1.5 Å, but the number of such events is insignificant and not shown in the plot. We note that the above result of the D−W_0 bond retaining its initial vibrational energy suggests the difficulty of collisionally deexciting the vibrational motion of chemisorbed atoms by gas-phase atoms.

Figure 2 indicates that the reaction is dominated by those collisions in which the gas atom is approaching the adatom at a small impact parameter. For the surface with the Boltzmann distribution of D−W vibrational energies at 300 K, all reactive events occur inside a cone with the radius of ≈1.2 Å around the center atom on which the D atom is chemisorbed. The distribution is particularly heavy around 0.7 Å. The radius is significantly shorter than the halfway distance between the adjacent surface atoms (1.58 Å). This result indicates that as the gas atom approaches the surface, it tends to move toward the adatom site for reaction under the influence of surface atoms, which produce a repulsive wall and steer the incident atom in the direction of the adatom. The model thus recognizes the presence of a strong attractive interaction between the gas and adsorbed atoms, while the gas to surface atom interaction is dominated by weak attraction at long range, but strong repulsion at short range ($D_{OS} = 0.12$ eV).[17]

As noted above, the reaction probability for O(g) + D(ad)/W → OD(g) + W at the thermal conditions of $T_g = 1000$ K and $T_s = 300$ K is 0.120. However, the OD can bind to tungsten as well; that is, the formation of a bound state on the surface is possible: O(g) + D(ad)/W → OD(ad)/W. In fact, at the thermal conditions, the probability of OD/W formation is 0.034. We have followed trajectories representing these bound cases and found that they are trapped even at times as long as $t = 8$ ns, which we may regard permanently bound to the surface (i.e., adsorption).[17] The rest of the collisions are the nonreactive case in which the adatom remains in the D(ad)/W state throughout the collision. On the LEPS potential energy surface used for the present study, no evidence exists of other channels, such as the direct binding of O to an adjacent surface site. Although the present work is devoted to the reaction taking place at the fixed thermal conditions of $T_g = 1000$ K and $T_s = 300$ K, we

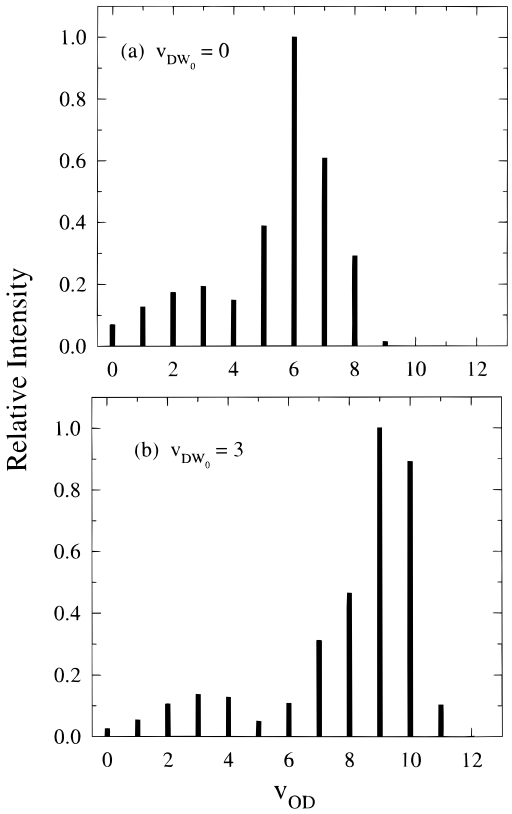

Figure 3. Relative intensity of the vibrational population distribution for the product OD for (a) $v_{DW_0} = 0$ and (b) $v_{DW_0} = 3$. Note that the OD vibrational energies corresponding to $v_{OD} = 5$, 7, and 9 are 1.69, 2.22, and 2.71 eV, respectively.

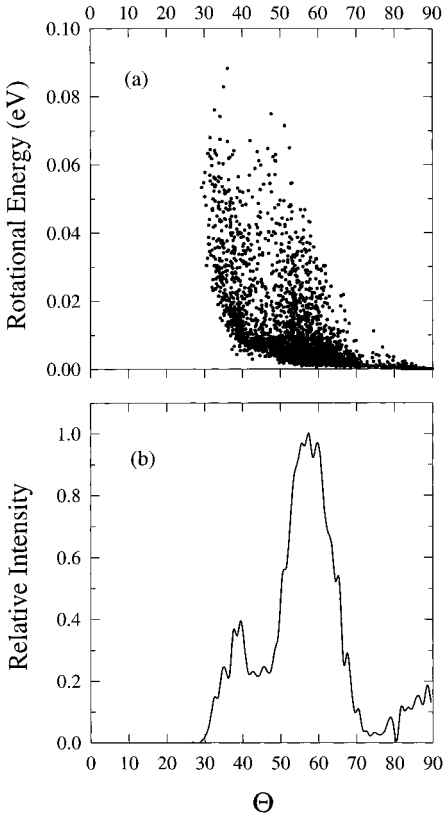

Figure 4. (a) Plot of the OD rotational energy as a function of Θ for $v_{DW_0} = 0$. (b) Distribution of Θ for $v_{DW_0} = 0$. Here Θ is the angle between the axis of rotation and the surface normal.

briefly discuss the dependence of the O(g) + D(ad)/W → OD(g) + W and → OD(ad)/W processes on the gas temperature. The probability of formation of the OD(ad)/W bound state is as high as 0.140 at $T_g = 300$ K, but rapidly decreases to 0.035 at $T_g = 900$ K, beyond which the probability varies slowly. On the other hand, the probability of OD formation rises slowly from 0.066 at $T_g = 300$ K to 0.120 at 900 K. Above 900 K, the increase is very slight. At $T_g = 1500$ K, the probabilities of OD(g) and OD(ad)/W formation are 0.130 and 0.020, respectively. A weak temperature dependence of the OD(g) formation indicates the presence of a low barrier on the potential energy surface. It is interesting to note that the activation energy for the OD(g) formation calculated from the plot of log P_{OD} versus $1/T$ is only 0.025 eV.

The distribution of OD vibrational energies and the variation of *b*-dependent reaction probabilities shown in Figure 2 indicate that the distribution of a large number of highly excited OD radicals at one end of the energy spectrum and the distribution of a small number of OD in low-lying vibrational states at the other end create conditions for a vibrational population inversion. Figures 3 shows the relative intensity of vibrational population distributions that are strongly inverted. Here, to mimic the quantum vibrational distribution, we have used a binning procedure of assigning quantum number v_{OD} corresponding to the calculated OD vibrational energy $E_{v,OD}$ through the relation $v_{OD} = \text{int}[E_{v,OD}/E_{vib}(v_{OD})]$, where the eigenvalue expression for $E_{vib}(v_{OD})$ is given above. For the D−W_0 vibration initially in the ground state, the maximum distribution occurs at $v_{OD} = 6$, which corresponds to the OD vibrational energy of 1.96 eV. The population is significant even for the vibrational level as high as 8 (see Figure 3a). Figure 3b shows that both the vibrational excitation and population inversion are very strong for the initial D−W_0 excitation corresponding to $v_{DW_0} = 3$. The maximum intensity occurs at $v_{OD} = 9$. The plot shows the excitation of product OD to the vibrational level as high as 11. Such high vibrational excitation is a characteristic of the ER mechanism. We note that if the Langmuir−Hinshelwood (LH) mechanism operates, the incident oxygen atom will also have to be chemisorbed, in which case the surface yields the chemisorption energy for O so the molecules formed could not be vibrationally excited. Since setting the initial D−W_0 vibrational energy of all 30 000 trajectories to $E^0_{v,DW_0} = 0.080$ eV at $T_s = 300$ K is equivalent to the Boltzmann sampling, the generation of such highly excited OD radicals at a convenient thermal condition offers important possibilities, such as utilizing excited OD in further reactions, which can then proceed at a greatly enhanced rate, or exploiting the population inversion for developing a chemical laser.

The amounts of energy deposited in the translational and rotational motions of OD are small, especially in the latter motion. Figure 4a displays the rotational energy as a function of Θ, where Θ is the angle between the axis of rotation and the surface normal at the turning point. The distribution of these angles provides the information on the rotational alignment of OD radicals receding from the surface. From the solution of the equations of motion we can determine this inclination angle Θ at the instant of impact (i.e., at the turning point). In a single-impact collision taking place on an extremely short time scale, we regard the angle at this instant to determine the rotational axis of the outgoing OD radical. The plot clearly shows that rotations, in contrast to vibrations, take up only a small fraction of the energy released in the reaction, but a more interesting result is a high distribution of angles in the range of $30 \leq \Theta \leq 70$. Figure 4b shows the relative intensity of the Θ distribution peaking at ≈60° for a near cartwheel-like rotation. Although

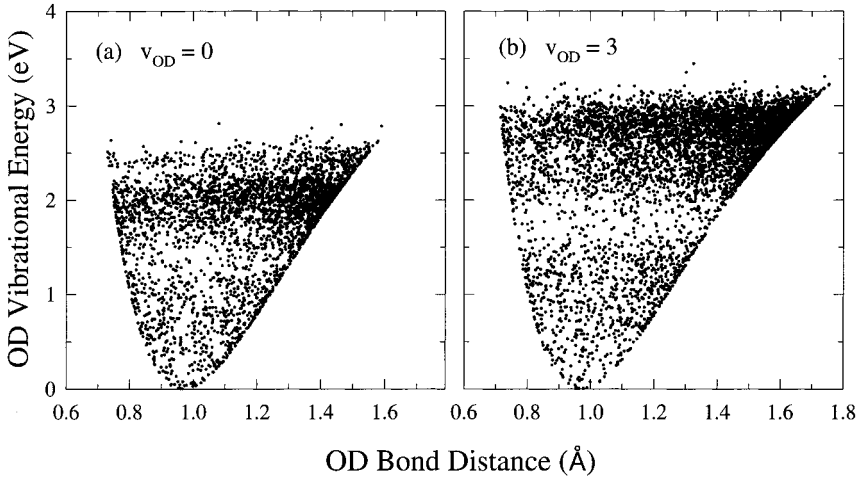

Figure 5. Plot of the OD vibrational energy versus the OD bond distance for the initial D−W_0 vibrational energies corresponding to (a) $v_{DW_0} = 0$ and (b) $v_{DW_0} = 3$.

its intensity is low, there are OD radicals whose rotational axis is actually parallel to the surface (see the distribution at $\Theta = 90°$ in Figure 4a). It is important to note the complete absence of OD with their rotational axis perpendicular to the surface, i.e., rotating like helicopters when they leave the surface.

The plot of the OD vibrational energy versus the OD bond distance reveals another interesting aspect of the present reaction system (see Figure 5). Again, we take the initial D−W_0 vibrational energies corresponding to $v_{DW_0} = 0$ and 3. Then we determine the OD bond distance of all reactive events at the instant when the receding OD radical has reached the fixed value of 30 Å from the surface. At such a large distance, the OD vibrational energy $E_{v,OD}$ in a given reactive event is fixed at its final value, but its bond distance can take any value between the two turning points around the equilibrium bond distance of 0.97 Å. The plots clearly display the occurrence of an inverted product vibrational distribution. An intriguing feature of this plot is the concentration of bond distances near the turning points, especially at the outer turning point. The concentration is particularly high for the $v_{DW_0} = 3$ case, where the product excitation is stronger. This is an important feature predicted by classical mechanics in that the classical particle has a zero velocity at the tuning point and therefore, on average, spends more time in the neighborhood of the turning points than in any other region. Because of the nature of anharmonicity of molecular vibration, the rebounding atoms spend more time near the outer turning point, where the CD intramolecular interaction is "softer". Hence, a larger number of reactive events are distributed at the outer turning point than the inner point.

To discuss the dynamics of energy flow and OD formation, we take a representative trajectory from the ensemble of subpicosecond reactive events for $v_{DW_0} = 0$. Figure 6a shows the evolution of the O···D and D−W_0 distances along with the collision trajectory. Here the collision trajectory is the O−surface distance *Z*, which correctly describes the gas−surface distance before the impact, but after the impact it represents the distance between O of the receding OD and the surface. The oscillation of the outgoing portion is due to the OD vibration. In this and all other subpicosecond reactive events, the D−W_0 distance diverges after the impact, reaching a value between 5 and 7 Å in about 0.3 ps. Although the D−W_0 distance diverges after the impact (see Figure 6a), the D−W_0 vibrational energy does not settle to the dissociation threshold until the time has reached ≈0.3 ps, although the CD vibrational energy has leveled off to the final value of 2.16 eV at a

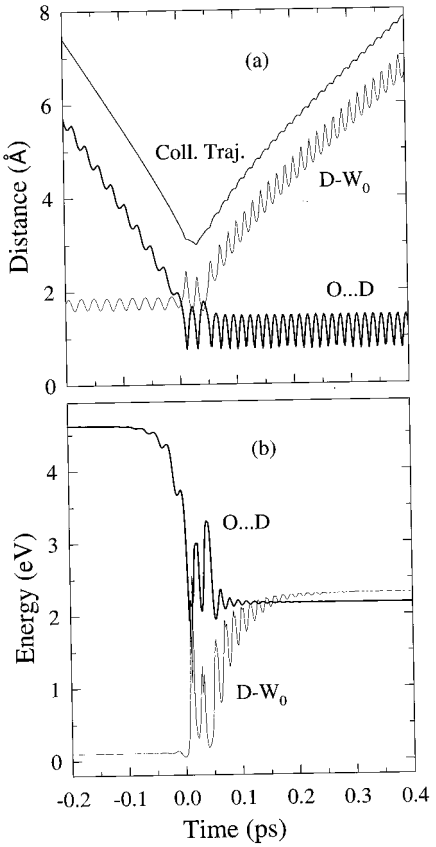

Figure 6. Dynamics of the reactive event representing the ensemble of single-impact collisions. Plot of the time evolution of (a) the collision trajectory, the O···D distance, and the D−W_0 distance and (b) the O···D and D−W_0 vibrational energies. After reaction, the O···D energy represents the vibrational energy of OD(g). After reaction, the D−W_0 vibrational energy remains at 2.30 eV, the dissociation threshold.

somewhat earlier time (see Figure 6b). The first minimum of the O···D distance represents the gas−surface impact, after which the trapped O atom undergoes a somewhat irregular vibration for a brief period before exhibiting a well-organized vibrational motion. Part of the energy supplied by the strong O···D interaction flows back and forth between O···D and D−W_0 in the short-lived complex O···D−W_0 before settling in the D−W_0 bond for its dissociation (see Figure 6b).

An important time scale in a molecular collision is the collision time (i.e., the duration of collision). However,

evaluation of this time scale is not a trivial task because it is often difficult to determine when the interaction begins and ends. As shown in Figure 5a, it does not appear possible to determine the start of collision from the time evolution of the collision trajectory, O···D distance, or D−W_0 distance. On the other hand, the start of collision is clearly noticeable in the evolution of the O···D and D−W_0 interaction energies shown in Figure 6b. The O···D interaction energy begins to decrease from the initial value of D_{OD} near $t = -0.1$ ps and then decreases very rapidly near $t = 0$ where the impact occurs, while the D−W_0 vibrational energy rises sharply. In all collisions, we find the O···D interaction energy starts to decrease from D_{OD} at a time very close to −0.10 ps. After the initial flow of energy from O···D to D−W_0, energy hops rapidly between the two bonds until the D−W_0 bond finally reaches its dissociation threshold near $t = +0.3$ ps, at which the D−W_0 bond dissociates and the O···D distance undergoes a well-organized vibration (see Figure 6a). Note that at this instant, the D−W_0 bond distance reaches $(5 + z_{e,DW_0})$ Å = 6.67 Å. In this representative case, therefore, the time spent by the gas atom in the interaction region from the start of collision at $t = -0.10$ ps to the end of interaction at $t = +0.30$ ps when the reaction is complete is 0.40 ps, which measures the duration of reaction. However, the reactive event really begins on impact, which occurs near $t = 0$, so the reaction time is 0.30 ps for this case. Figure 6b shows an efficient energy flow between the O···D and D−W_0 bond over the period of about 0.1 ps following the impact, with the net result of a large amount of energy accumulating in the D−W_0 bond. We have checked many reactive trajectories and found that although time scales differ for different trajectories, the qualitative picture of time evolution for all subpicosecond trajectories remains unchanged with the reaction beginning near $t = 0$ and ending some time between $t = 0.2$ and 0.4 ps.

At the beginning of collision, an incident gas atom carrying a large amount of the O···D interaction energy in addition to the collision energy E impinges on the surface and meets a chemisorbed D atom in the potential well. It first undergoes inelastic interaction with the adatom on the repulsive wall of the O···D interaction potential. When the O···D interaction loses energy to the D−W_0 vibration, the incident gas atom falls into the O···D potential well. When O···D stabilizes to OD, it desorbs with an available energy of $D_{OD} + E^0_{v,DW_0} + E - D_{DW_0}$). Since E^0_{v,DW_0} and E are normally much smaller than other energy terms in the available energy, the maximum energy available for desorbing OD is largely determined by the difference between the attractive energy D_{OD} and the chemisorption energy D_{DW_0}.

In the representative case considered in Figure 6, after a brief pause at the upper region, the gas atom falls into near the halfway depth of the well. The sharp rise and fall of the O···D and D−W_0 energies during the impact clearly indicate an efficient flow of energy from the newly formed energy-rich O···D bond to the weakening D−W_0 bond in a short-lived transitory state O···D−W_0 on the surface as a result of a strong collision between O and D. That is, at the impact, the transfer of a large amount of energy ($\gg kT$) occurs in a single-step process rather than a ladder-step process in which the O···D interaction would lose its energy to the D−W_0 bond in a series of small steps.

We now consider a representative reactive event for multiple-impact collisions taking place on a longer time (picosecond) scale. Although only about 5% of the reactive events occur through such collisions, their trajectories reveal some interesting aspects of the complex-mode collision, whose time evolution

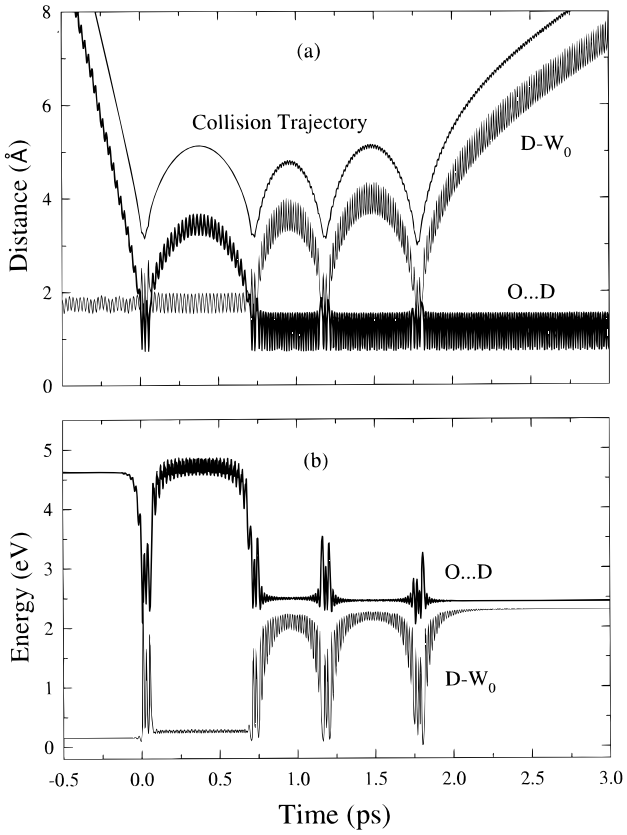

Figure 7. Dynamics of the reactive event representing multiple-impact collisions. The curves are displayed as in Figure 6.

of distances and energies differs significantly from that of the direct-mode case displayed in Figure 6. The four-impact case representing such long-time events is shown in Figure 7. The variation of the O···D and D−W_0 distances indicates the collision lasting about 2 ps. We first notice that the collision trajectory between the first and second turning points undergoes a smooth oscillation compared to the remaining portion after the second turning point. This smooth variation is due to the situation that the deuterium is still rather tightly bound to the surface, gaining only a small amount of energy from the gas atom. As shown in Figure 7b, there is efficient energy transfer from O···D to D−W_0 on the initial impact near $t = 0$, but unlike in the single-impact case, the D−W_0 bond now returns most of its vibration energy to O···D and remains in a low-energy state until $t \approx +0.7$ ps, during which the O atom undergoes a large-amplitude excursion into the gas phase but fails to escape. During this period, the D−W_0 is nearly free from the gas atom, which is at a large distance from the surface. The rebounding O atom spends a relatively long time near the apex, where the kinetic energy vanishes, of the barely trapped trajectory and then becomes attracted back to the adatom atom, suffering a second impact near $t = +0.7$ ps. At this impact, the D−W_0 bond in O···D−W_0 gains a large amount of energy. Thus, only after pounding the adatom twice, the gas atom is able to transfer a significant amount of energy to the D−W_0 bond and begins a serious negotiation with the D−W_0 vibration for bond dissociation. Figure 7a clearly shows that the vibrational motion of O···D in the time range between the second and third impacts is well organized, representing a rather stable O···D state (see the O···D distance in Figure 7a and the O···D energy in Figure 7b). Now O···D instead of D alone tends to recede from the surface, and the receding O···D undergoes a large-amplitude excursion from the surface, but it just fails to escape. The O···D is attracted back to the surface at $t = +1.2$ ps and suffers a

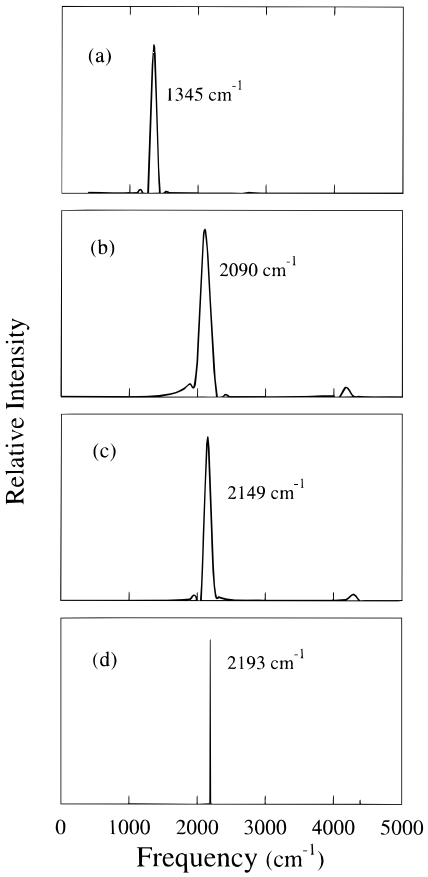

Figure 8. Power spectra of the O···D vibration (a) between the first and second turning points, (b) between the second and third turning points, (c) between the third and fourth turning points, and (d) after the fourth turning point (i.e., for the free OD).

third impact. From the third impact to the fourth (and final) impact, O···D repeats the time evolution which is nearly identical to that in the previous range. At the last two turning points, there is a rapid flow of energy between O···D and D−W_0, with the latter vibration making a small net gain of energy at each impact, thus progressing toward the dissociation threshold. After the fourth impact, the D−W_0 vibrational energy finally reaches the threshold at $t \approx +2.2$ ps, where the O···D energy levels off to the final OD vibrational energy of 2.43 eV, corresponding to CD vibrational level 8. Thus, the reaction time of this representative case is about 2.2 ps. The O···D energy curve plotted in Figure 7b shows that the O···D bond after the second impact near $t = +0.7$ ps is essentially identical to the latter energy, indicating that the extent of the product excitation of OD has already been decided at an early stage of the reaction course.

Finally, we note the vibration of the O···D distance after each impact as shown in Figure 7a. Even between the first and second impacts, O···D undergoes a low-frequency vibration, while the oxygen atom makes a large-amplitude excursion. The Fourier transform of the O···D distance in this time interval ($t = 0-0.7$ ps) gives a vibrational frequency of 1345 cm^{-1}, which indicates the O···D interaction lying near the top of the potential well (see Figure 8a). But the O···D vibrational frequencies for the trapped state between the second and third impacts ($t = 0.7-1.2$ ps) and between the third and fourth impacts ($t = 1.2-1.8$ ps) are 2094 and 2149 cm^{-1}, respectively, which correspond to the energy states near the halfway of the well depth. Therefore, the latter two states represent a large drop of the O···D energy from the top of the potential well, as in the single-impact case. In the product state (i.e., after the fourth impact), OD vibrates at a well-defined frequency of 2193 cm^{-1}, which is very close to the $v_{OD} = 6 \rightarrow 5$ frequency. The latter spectrum is the Fourier transform of the O···D vibration for $t > 2.2$ ps, when OD has receded a large distance from the surface. The broadness of the first three peaks (see Figure 8a,b,c) is the result of sampling a limited number of O···D vibrations between the turning points in the Fourier procedure. The appearance of a low-intensity peak for the overtone vibration is seen in each case. The gradual blue-shift of frequency displayed in Figure 8 presents a clear picture of the "birth" of a chemical bond in multiple-impact collisions where the lifetime of a gas−adatom complex on the surface is reasonably long. Although they constitute only about 5% in the present system, multiple-impact collisions are therefore both important and interesting as they reveal subtle aspects of the dynamics of reaction taking place at the gas−surface interface. In the present complex-mode collision, unlike in the direct-mode collision considered in Figure 6, the gas atom stays on the surface for a considerable duration (>1 ps), forming a gas−adatom complex, a precursor state.[26] However, its residency is no more than several picoseconds, which is not long enough for the incident gas atom to equilibrate to the surface so it cannot be considered to follow the LH type. In fact, Pedan and co-workers have considered a gas−surface reaction to follow the ER mechanism as long as its time scale is less than 10 ps.[27]

IV. Concluding Comments

We have shown the production of highly excited OD radicals in the reaction of gas-phase atomic oxygen with chemisorbed deuterium on a room-temperature tungsten surface taking place on a potential energy surface constructed using a modified LEPS procedure. The temperature of incident gas atoms is maintained at 1000 K. Nearly 95% of the reactive events occur on a subpicosecond scale through a single-impact collision of the gas atom with the adatom. A major portion of the reaction energy goes into the product vibration. The distribution of product vibrational energies is nonstatistical, showing a strong population inversion, with the maximum intensity appearing at the vibrational energy corresponding to vibrational level 6. Some reactive events lead to excitation as high as level 8. Such high vibrational energy and inverted population distribution suggest that the D extraction reaction by O on a tungsten surface can be used to initiate further reactions involving OD radicals, in which case the reaction can proceed at an enhanced rate. Furthermore, these results suggest that such a surface-catalyzed reaction can be developed as the basis for an OD chemical laser. The results of vibrational energy distribution, vibrational population inversion, and time evolution of energies during the course of reaction are important in elucidating the fundamental role played by the metal surface in the OD formation. Since the problem of vibrational population inversion is of practical importance in reaction dynamics, designing new experiments for further studies of this aspect is desirable.

Although the number of complex-mode collisions is small, such reactive events that occur on a picosecond scale show a clear picture of the dynamic behavior of a weakly bound O···D on the surface and gradual strengthening of the O···D bond before forming a stable OD radical.

Acknowledgment. The computational part of this research was supported by a NSF Advanced Computing Resources grant (CHE-890039P) at the Pittsburgh Supercomputing Center. I would like to thank Professor J. Ree for valuable discussions.

References and Notes

(1) Tamm, P. W.; Schmidt, L. D. *J. Chem. Phys.* **1971**, *54*, 4775.
(2) Anders, L. W.; Hansen, R. S.; Bartell, L. S. *J. Chem. Phys.* **1973**, *59*, 5277.
(3) McCreery, J. H.; Wolken, G., Jr. *J. Chem. Phys.* **1977**, *66*, 2316.
(4) Elkowitz, A. B.; McCreery, J. H.; Wolken, G., Jr. *Chem. Phys.* **1976**, *17*, 423.
(5) Barnes, M. R., Willis, R. F. *Phys. Rev. Lett.* **1978**, *41*, 1729.
(6) Hall, R. I.; Cadez, I.; Landau, M.; Pichou, F.; Schermann, C. *Phys. Rev. Lett.* **1988**, *60*, 337.
(7) Eenshuistra, P. J.; Bonnie, J. H. M.; Los, J.; Hopman, H. J. *Phys. Rev. Lett.* **1988**, *60*, 341.
(8) Rettner, C. T.; Schweizer, E. K.; Mullins, C. B. *J. Chem. Phys.* **1989**, *90*, 3800.
(9) Kuipers, E. W.; Vardi, A.; Danon, A.; Amirav, A. *Phys. Rev. Lett.* **1991**, *66*, 116.
(10) Kratzer, P.; Brenig, W. *Surf. Sci.* **1991**, *254*, 275.
(11) Shin, H. K. *J. Chem. Phys.* **1992**, *96*, 3330.
(12) Jackson, B.; Persson, M. *J. Chem. Phys.* **1992**, *96*, 2378.
(13) Jackson, B.; Persson, M. *Surf. Sci.* **1992**, *269*, 195.
(14) Schermann, C.; Pichou, F.; Landau, M.; Cadez, I.; Hall, R. I. *J. Chem. Phys.* **1994**, *101*, 8152.
(15) Xu, W.; Adams, J. B. *Surf. Sci.* **1994**, *319*, 45.
(16) Shin, H. K. *Chem. Phys. Lett.* **1995**, *244*, 235.
(17) Ree, J.; Kim, Y. H.; Shin, H. K. *J. Phys. Chem.* **1997**, *101*, 4523.
(18) Nordlander, P.; Holloway, S.; Norskov, J. K. *Surf. Sci.* **1984**, *136*, 59.
(19) Christmann, K. *Surf. Sci. Rep.* **1988**, *9*, 1.
(20) Adelman, S. A.; Doll, J. D. *J. Chem. Phys.* **1976**, *64*, 2375.
(21) Adelman, S. A. *J. Chem. Phys.* **1979**, *71*, 4471.
(22) Adelman, S. A. *Adv. Chem. Phys.* **1980**, *44*, 143.
(23) Tully, J. C. *J. Chem. Phys.* **1980**, *73*, 1975.
(24) Ree, J.; Kim, Y. H.; Shin, H. K. *J. Chem. Phys.* **1996**, *104*, 742.
(25) Huber, K. P.; Herzberg, G. *Constants of Diatomic Molecules*; Van Nostrand Reinhold: New York, 1979.
(26) Harris, J.; Kasemo, B. *Surf. Sci.* **1981**, *105*, L281.
(27) Peden, C. H.; Goodman, D. W.; Weisel, M. D.; Hoffmann, F. M. *Surf. Sci.* **1991**, *253*, 44.